Preparation and Characterization of Chromium(III)-Activated Yttrium Aluminum Borate: A New Thermographic Phosphor for Optical Sensing and Imaging at Ambient Temperatures

Sergey M. Borisov,*,† Karl Gatterer,‡ Brigitte Bitschnau,‡ and Ingo Klimant†

Institute of Analytical Chemistry and Food Chemistry, Graz University of Technology, Stremayrgasse 16, A-8010, Graz, Austria, and Institute of Physical and Theoretical Chemistry, Graz University of Technology, Rechbauerstrasse 12, A-8010, Graz, Austria

Received: February 24, 2010; Revised Manuscript Received: March 22, 2010

A new thermographic phosphor based on chromium(III)-doped yttrium aluminum borate (YAB) is obtained as single crystals by high temperature flux growth and as a microcrystalline powder via solution combustion synthesis. The phosphor is excitable both in the blue (λ_{max} 422 nm) and in the red part of the spectrum (λ_{max} 600 nm) and shows bright NIR emission. The brightness of the phosphor is comparable to that of a well-known lamp phosphor Mn(IV)-doped magnesium fluorogermanate. At ambient temperatures, the Cr(III)-doped YAB shows high temperature dependence of the luminescence decay time, which approaches 1% per deg. The material shows no decrease in luminescence intensity at higher temperatures. The new phosphor is particularly promising for applications in temperature-compensated optical chemosensors (including those based on NIR-emitting indicators) and in pressure-sensitive paints.

Introduction

Temperature is undoubtably one of the most important parameters to know in various fields of science and technology, and in everyday life. Contactless sensing is particularly attractive for various applications where invasiveness is undesirable. Major contactless techniques include optical pyrometry, IR thermography, and phosphor thermometry. Among them, optical pyrometry is only suitable for measurements at high temperatures (>600 °C). On the other hand, much lower temperatures and particularly those around room temperature are of great practical interest. For example, precise temperature determination is essential in marine research,[1,2] geochemical studies,[3] medicine,[4,5] and aeronautics,[6] to mention only a few areas. Moreover, temperature is a key parameter in optical sensing since the response of virtually all such sensors is temperature dependent. IR thermography has become very widespread but is still rather expensive and may suffer from various artifacts.[7] Luminescent temperature-sensitive materials represent a promising alternative here. They respond to temperature by altering the luminescence intensity or decay time. Thermographic phosphors are well established and have been in use for decades.[8] Some of them find application in commercial devices (e.g., fiber-optic thermometers from LumaSense technologies, www.lumasenseinc.com). However, most of the thermographic phosphors are intended for sensing high temperatures and become practically useless at ambient conditions.[9] The suitable phosphors for RT sensing include manganese(IV)-doped magnesium fluorogermanate Mg_4FGeO_6,[10,11] chromium(III)-doped yttrium−aluminum garnet $Y_3Al_5O_{12}$,[12] aluminum oxide (ruby),[13,14] spinel $MgAl_2O_4$,[15] and yttrium−aluminum perovskite $YAlO_3$,[16] as well as europium(III)-doped lanthanum oxysulphide La_2O_2S.[17,18] Some other phosphors also have been proposed.[19] The limitations of these phosphors include rather low temperature sensitivity and/or insufficient luminescence brightness. Apart from thermographic phosphors, organometallic complexes which possess temperature-dependent luminescence were found to be very useful probes. Recently, they became increasingly popular and were applied in dually sensing materials[20−26] and pressure-sensitive paints.[27−31] Such materials usually rely on the use of ruthenium(II) polypyridyl complexes[22,30,32] and europium(III) tris-β-diketonates.[21,26,28,33,34] Generally, these temperature probes suffer from photostability issues, decreased luminescence intensity at higher temperatures, and pronounced cross-sensitivity to oxygen so that their immobilization in gas-blocking polymers such as polyacrylonitrile is usually essential.[32] Some temperature-sensitive fluorophores also were reported[35,36] but they are less convenient due to measurements of fluorescence intensity and not the decay time.

Evidently, state of the art thermographic phosphors and luminophores have their limitations and more advanced materials are highly desired. An "ideal" luminescent material for sensing temperature should fulfill the following requirements: (i) have high brightness; (ii) possess excitation in the visible or NIR part of the spectrum to minimize autofluorescence interferences; (iii) have high-temperature sensitivity in the desired range; (iv) be photostable; (v) have negligible cross-sensitivity to other analytes such as, e.g. oxygen; and (vi) be commercially available or simple to manufacture. Very often relatively long luminescence decay times (>1 μs) are desirable in order to enable lifetime interrogation. In this contribution we will demonstrate that chromium(III)-doped yttrium aluminum borate (YAB) fulfills all these requirements and is, therefore, a thermographic phosphor of choice for sensing and imaging at ambient temperatures.

Experimental Section

Materials. Yttrium oxide (99.99%), gadolinium nitrate hexahydrate (99.9%), chromium(III) nitrate nonahydrate (99%),

* To whom correspondence should be addressed. E-mail: sergey.borisov@tugraz.at.

† Institute of Analytical Chemistry and Food Chemistry, Graz University of Technology.

‡ Institute of Physical and Theoretical Chemistry, Graz University of Technology.

10.1021/jp1016467
Published on Web 04/14/2010

and molybdenum(VI) oxide (99.5+%) were obtained from Aldrich (www.sigmaaldrich.com), aluminum nitrate nonahydrate (99+%), yttrium nitrate hexahydrate (99.9%), urea (99.5%), and chromium(III) oxide (99,997%) were from Fischer Scientific (www.fishersci.com), aluminum oxide (>99%) was from Merck (www.merck.de), hydrogel D4 was from AdvanSourse biomaterials (www.advbiomaterials.com), boron trioxide (>99%), potassium hydroxide, and potassium sulfate (99+%) were from Fluka (www.sigmaaldrich.com), and boric acid (99.99%) was from ABCR (www.abcr.de). Mn(IV)-doped magnesium fluorogermanate was generously provided by OSRAM (Schwabmünchen, Germany).

Microcrystalline powders of chromium(III)-doped YAG $Y_3Al_{4.8}Cr_{0.2}O_{12}$, spinel $MgAl_{1.96}Cr_{0.04}O_4$, and ruby $Al_{1.96}Cr_{0.04}O_3$ were obtained from the nitrates and urea with the solution combustion technique. The powders were sintered for 24 h at 1100 °C in air.

The luminescent beads of ruthenium(II) tris-1,10-phenanthroline in poly(acrylonitrile) (=Ru-phen/PAN) and europium (III) tris(2-thenoyltrifluoroacetonato)-4-(4,6-di(indazol-1-yl)-1,3,5-triazin-2-yl)-*N*,*N*-diethylbenzenamine in poly(styrene-*block*-vinylpyrrolidone) ($Eu(tta)_3$DEADIT/PS-PVP) were prepared as described elsewhere.[22,37]

Preparation of Cr(III)-Doped YAB Single Crystals. The Cr(III)-doped YAB crystals were obtained by high-temperature flux growth technique The appropriate amounts of the yttrium oxide, aluminum oxide, boron trioxide, and chromium(III) oxide were homogenized in a mortar and mixed with a flux system consisting of potassium sulfate and molybdenum(VI) oxide. The ratio of oxides to flux was 2:3 (w/w). The mixture was loaded in platinum crucibles and melted in a front-loaded electric resistance furnace, equipped with a programmable temperature controller. The temperature program consisted of heating to 1120 °C at 300 deg/h, keeping that temperature for 3 h, and then slowly cooling to 900 °C at a rate of 1 deg/h. Upon removing the flux by boiling in concentrated potassium hydroxide (c = 8.0 M) YAB crystals (100 μm−10 mm) were obtained. Whenever necessary the crystals were ground to microcrystalline powders in an agate mortar.

Preparation of Cr(III)-Doped YAB Microcrystalline Powders. Microcrystalline YAB powders were synthesized employing the solution combustion method with urea as a fuel. Typically, 5 mmol (1.915 g) of yttrium nitrate hexahydrate, 13.5−14.85 mmol (5.064−5.570 g) of aluminum nitrate nonahydrate, 0.25−1.5 mmol (0.100−0.600 g) of chromium nitrate nonahydrate, 20 mmol (1.236 g) of boric acid, and 100 mmol (6 g) of urea were dissolved in 10 mL of deionized water. The solution was heated in a resistance furnace to 500 °C (heating rate ~20 deg/min) and this temperature was maintained for 15 min. The obtained raw material was milled in an agate mortar and sintered in a porcelain crucible for 24 h at 1100 °C in air. The powder was ground in a ball mill to result in 2.6 ± 0.5 μm microcrystalls.

Microcrystalline Cr(III)-doped gadolinium aluminum borate (GAB) powder was obtained in a similar manner, where gadolinium(III) nitrate was used instead of yttrium(III) nitrate.

Measurements. Emission and excitation spectra were acquired on a Hitachi F-7000 fluorescence spectrometer (www.hitachi.com) equipped with a red-sensitive photomultiplier R 928 from Hamamazu (www.hamamatsu.com). The emission spectra were corrected for the sensitivity of the PMT as described previously.[38] The emission and excitation spectra were acquired for the phosphor powders fixed in a homemade cell positioned at 60° toward the excitation light.

Luminescence phase shifts were measured with a two-phase lock-in amplifier (SR830, Standford Research Inc., www.thinksrs.com). The phosphors were (crystals or microcrystalline powders) placed in a homemade cuvette and excited with the light of a 405 nm LED (www.roithner-laser.com) filtered through a BG-12 glass filter (www.schott.com). The luminescence was detected with a photomultiplier tube (H5701-02, Hamamatsu, www.sales.hamamatsu.com) after passing an RG 630 filter from Schott. A bifurcated fiber bundle was used to guide the excitation light to the probe and to guide back the luminescence. Modulation frequencies of 1 and 2 kHz were used for Cr(III)-doped YAB and Cr(III)-doped GAB, respectively. The temperature was controlled by a cryostat ThermoHaake DC50.

The luminescence decay profiles were acquired on a BMG Labtech FLUOstar Optima microplate reader (www.bmg-labtechnologies.com). The powder was excited at 405 nm and a long-pass RG 9 filter was used for the emission.

Imaging in the time domain was performed with a gated SensiCAM camera (cooled CCD-chip, 640 × 480 pix, black and white, www.pco.de). A high-power 405-nm LED (www.roithner-laser.com) was used as an excitation source.

The X-ray powder diffraction data were collected with a laboratory powder diffractometer (Philips X-Pert) from a flat sample (Bragg−Brentano geometry) with use of Cu Kα radiation. The measurements were carried out from 10° to 95° 2θ, with a step width of 0.02° and a constant counting time of 5 s per step. Rietveld refinement was performed with FULLPROF.[39,40] The starting model for structural parameters was taken from ICSD, FIZ Karlsruhe ($YAl_3(BO_3)_4$, 91962,[41] YBO_3, 84653).[42] A Pseudo-Voigt profile shape function was used. The background was refined with a polynomial function. The amount of preferred orientation was corrected by the March−Dollase function.

Results and Discussion

Phosphor Preparation and Crystal Structure. Yttrium aluminum borate (YAB) is isostructural with the mineral Huntite and has a trigonal crystal structure of *R*32 space group.[43] Both trivalent rare-earth and transition metal ions (e.g., chromium(III)) can be doped into the material, where rare-earth ions then occupy yttrium sites and transition metal ions replace aluminum(III) on sites of octahedral symmetry.[44] It is known that concentration quenching of luminescence in this structure is usually lower than in other solid hosts, thus allowing higher dopant levels.[45]

Two different techniques were used to obtain Cr(III)-doped YAB, namely flux growth and the solution combustion method. In the first method, Cr(III)-doped YAB crystals are grown from the solution in high-temperature flux of potassium molybdate. High-temperature top-seeded solution growth technique can also be used.[46,47] The YAB crystals obtained by this method have high purity as demonstrated by powder diffraction patterns (Figure 1). On the other hand, the flux growth has a number of limitations. First, the method is time-consuming due to slow cooling required during crystal growth (1 deg/h) and has a laborious extraction procedure (dissolving of the flux in concentrated potassium hydroxide). Second, micrometer-sized powders are strongly preferred for practical applications and grinding of the crystals becomes necessary. Third, the amount of dopant cannot be controlled precisely since some of the chromium(III) ions may remain in the flux. Therefore, the solution combustion method represents a promising alternative to the flux growth technique. Microcrystalline powders are easily obtained by combustion of the solutions containing respective

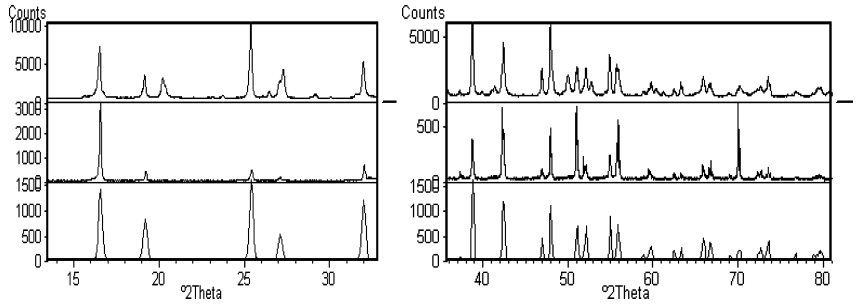

Figure 1. Powder diffraction patterns for YABs: (a) obtained by the combustion method with subsequent 24 h sintering at 1100 °C, impurity of about 4% YBO_3; (b) flux growth crystals (5% Cr(III) in the oxide mixture), powder pattern shows preferred orientation; (c) simulated powder diffraction pattern of single phase YAB.

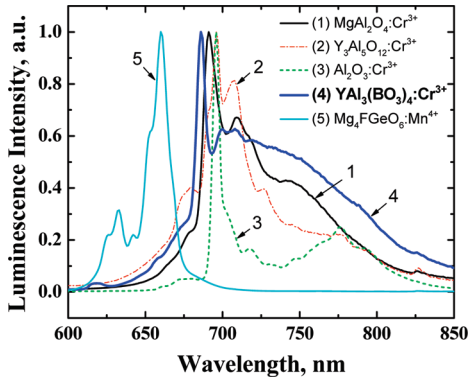

Figure 2. Emission spectra of the Cr(III)- and Mn(IV)-doped thermographic phosphors (λ_{exc} 405 nm).

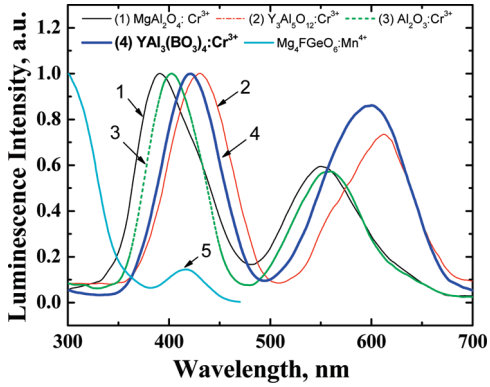

Figure 3. Excitation spectra of the Cr(III) and Mn(IV) thermographic phosphors.

metal nitrates, boric acid, and urea (used as a fuel) with subsequent 24 h sintering at 1100 °C. The powder diffraction patterns (Figure 1) demonstrate that the phosphor obtained with the combustion method has lower purity. The impurity is attributed to the presence of about 4% yttrium borate[48] quantified by Rietveld refinement. In fact, Maia et al.[49] have shown that YABs obtained by the sol−gel and the polymeric precursor methods contain YBO_3 phase as an impurity. The authors have demonstrated that it is possible to obtain pure microcrystalline powders using the polymeric precursor method with subsequent sintering at 1150 °C.

Photophysical Properties. The emission and luminescence excitation spectra for the Cr(III)-doped YAB are shown in Figures 2 and 3, respectively. The phosphor has an intense broad luminescence in the NIR region associated with the $^4T_2 \rightarrow {}^4A_2$ transition and an additional sharp R-line associated with the $^2E \rightarrow {}^4A_2$ transition. The schematic configuration coordinate diagram (see Figure 4b) highlights the zero-phonon nature of the sharp transition from the ^2E state as compared with the broad

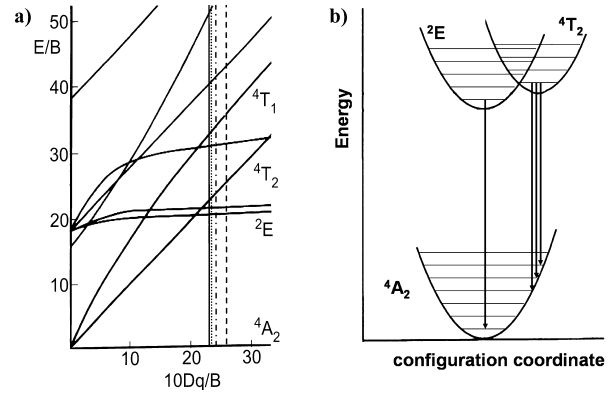

Figure 4. (a) Tanabe−Sugano diagram of Cr(III) in octahedral environments. Only relevant energy levels are assigned. The 10 Dq/B values of $YAl_3(BO_3)_4:Cr^{3+}$ (solid), $Y_3Al_5O_{12}:Cr^{3+}$(dotted), $MgAl_2O_4:Cr^{3+}$ (dot and dash), and $Al_2O_3:Cr^{3+}$ (dashed) are indicated. (b) Configuration coordinate diagram (not to scale) of Cr(III) in octahedral environments.

vibronic transition from the $^4T_2$ state, which is placed toward lower energy. In the Tanabe−Sugano diagram for Cr(III) in octahedral crystal fields (see Figure 4a) the 10 Dq/B values for all investigated Cr(III) containing phosphors are indicated. All hosts provide 10 Dq/B ratios which have the ^2E state as the lowest lying emitting state. It is evident that for the YAB the energy difference between the two emitting states (^2E and $^4T_2$) is the smallest. Excitation of the Cr(III)-doped YAB is attributed to the $^4A_2 \rightarrow {}^4T_2$ and $^4A_2 \rightarrow {}^4T_1$ transitions with band maxima at 421 and 599 nm, respectively. Therefore, the Cr(III)-doped YAB can be excited both in the blue and in the red part of the spectrum, which is nicely compatible with the emission of the 635 nm red laser diode. Notably, among thermographic phosphors only Cr(III)-doped $Y_3Al_5O_{12}$ shows similar spectral features (Figure 3). It is evident that other thermographic phosphors such as Cr(III)-doped $MgAl_2O_4$ and Al_2O_3 as well as Mn(IV)-doped Mg_4FGeO_6 cannot be efficiently excited in the red part of the spectrum (Figure 3).

Figure 5 shows the dependences of the luminescence decay time and the luminescence intensity on the amount of Cr(III) ions which substitute Al(III) in YAB. Evidently, concentration quenching is observed even at rather low Cr(III) doping levels, which is indicated by the decrease in luminescence decay time. However, the luminescence intensity does increase with increasing of Cr(III) doping since more light can be absorbed by the phosphor. At higher levels of the activator concentration quenching becomes predominant and the intensity decreases after more than 4% of aluminum ions are substituted by chromium ($x = 0.12$). Thus, YABs where 2−4% of Al(III) is substituted by Cr(III) can be a good compromise between luminescence brightness and the degree of concentration quenching.

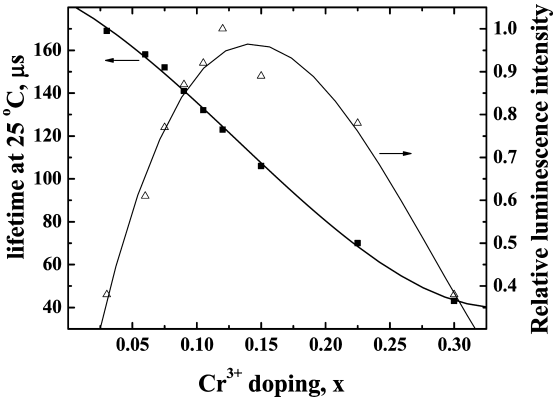

Figure 5. Concentration quenching of the luminescence intensity and decay time of the $YAl_{3-x}Cr_x(BO_3)_4$ microcrystalline powders.

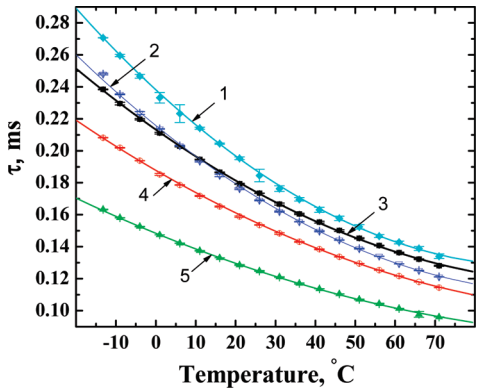

Figure 6. Temperature dependence of the luminescence decay time for Cr(III)-doped YAB phosphors: (1) crystals obtained by high-temperature solution growth (5% Cr(III) in the oxide mixture); (2) ground crystals; and (3, 4, 5) microcrystalline powders obtained via combustion with 1%, 2.5%, and 4% of Cr(III), respectively.

Temperature Sensitivity. The luminescence decay time of Cr(III)-doped YAB was found to be highly temperature-dependent, which is the basis for its use as a thermographic phosphor (Figure 6). Generally, the crystals obtained by top-seeded solution growth show the longest decay times and the highest temperature sensitivity approaching 1% of the lifetime change per 1 deg. For all Cr(III)-doped YABs, temperature sensitivity is the highest at ~0 °C and becomes lower if the temperature increases. The decay time becomes slightly shorter if the crystals are ground into powder (Figure 6). This common phenomenon originates from inner defects in the crystal structure which accumulate during grinding. Notably, the lifetime for the powders obtained via the combustion route is generally lower than that for the crystals and is less temperature-dependent, which is attributed to the impurity of yttrium borate and inner defects in the crystal structure. As demonstrated by Maia et al.,[49] YABs of higher purity can be obtained using the polymer precursor method. Such YABs are likely to show improved photophysical performance (longer decay times, higher brightness, and temperature sensitivity).

Temperature dependence of the luminescence intensity of Cr(III)-doped YAB is shown in Figure 7. Evidently, temperature significantly affects the intensity of the R-line associated with the $^2E \rightarrow {}^4A_2$ transition, which decreases with temperature. On the other hand, broad NIR luminescence associated with the $^4T_2 \rightarrow {}^4A_2$ transition remains relatively constant and even increases with temperature. The isosbestic point at ~738 nm is explained by the thermal population of the $^4T_2$ emitting state from the metastable ^2E state. As has been shown in Figure 4

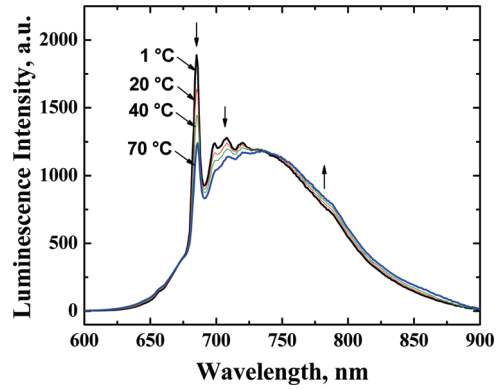

Figure 7. Temperature dependence of the luminescence intensity for Cr(III)-doped YAB (2.5% Cr(III), combustion method).

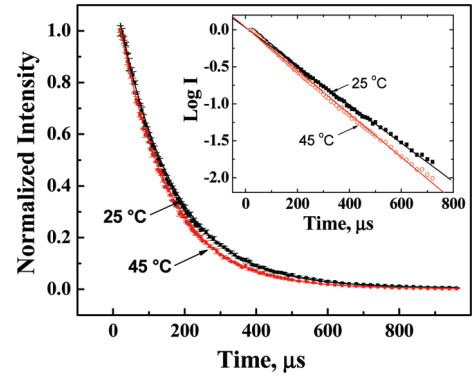

Figure 8. Time dependence of the emissions for Cr(III)-doped YAB (2.5% Cr(III), combustion method). The insert shows a representation with a logarithmic scale. Lines represent a fit via monoexponential decay model (main graph) and a linear fit (the insert).

for the YAB host these two states are closest in energy. As demonstrated by Dominiak-Dzik et al.,[50] at lower temperatures (77 K) the broad NIR emission further decreases in intensity accompanied by the increase of intensity for the R-line. Notably, the overall decrease in luminescence intensity on going from 1 to 70 °C is negligible and does not exceed 0.2%. Thus, the S/N ratio for Cr(III)-doped YAB remains constant in this temperature range. On the contrary, if luminescent metal−ligand complexes are used as temperature probes the decrease in luminescence intensity is usually very pronounced and is often as high as several percent per degree.[34] This results in much lower S/N ratios at higher temperatures. Despite the fact that Cr(III)-doped YAB emits from both ^2E and $^4T_2$ states, the luminescence decay profiles are virtually monoexponential (correlation coefficient >0.9996), Figure 8. Moreover, temperature does not affect the form of the decay curve. The decay times obtained in the time domain and in the frequency domain are virtually identical, e.g. 154 and 155 μs for the YAB containing 2.5% Cr(III), for the time domain and frequency domain measurements, respectively.

Cr(III)-Doped YAB vs Other Thermographic Phosphors and Metal−Ligand Complexes. The luminescence brightness of the Cr(III)-doped YAB microcrystalline powder (2.5% Cr(III)) was estimated from the corrected emission spectrum under 405 nm excitation. It was compared to the brightness of other thermographic phosphors which are also excitable at this wavelength (Figure 3). For all the phosphors, 20 mg of a microcrystalline powder (2−5 μm) was dispersed in 1 mL of poly(ethylene glycole) and the suspension was interrogated in a fluorescence spectrometer. The relative brightnesses were determined to be 1, 0.61, 0.69, 0.42, and 0.16 for Mn(IV)-doped Mg_4FGeO_6, Cr(III)-doped $YAl_3(BO_3)_4$, Al_2O_3, $MgAl_2O_4$, and

TABLE 1: Properties of the Visible Light-Excitable Luminescent Probes for Room Temperature Thermometry

temp probe	λ_{exc}, nm	τ at 1 °C, μs	τ at 60 °C, μs	sensitivity at 1 °C, % τ/K	sensitivity at 60 °C, % τ/K	brightness at 1 °C	brightness at 60 °C	photostability	cross-sensitivity to O_2	refs
Ru-phen/PAN	424, 449	4.3	2.9	0.55	0.82	0.42[a]	0.16[a]	good	low	22
Eu(tta)$_3$DEADIT/PS	413	483	190	0.40	4.00	0.9[b]	0.25[b]	poor	significant	33
Mg_4FGeO_6:Mn(IV)	417	3610	3190	0.19	0.22	1	0.98	very good	negligible	11
Al_2O_3:Cr(III)	402, 559	3980	3380	0.25	0.30	0.34	0.33	very good	negligible	14
$MgAl_2O_4$:Cr(III)	391, 551	9830	7610	0.38	0.49	0.32	0.29	very good	negligible	14
$Y_3Al_5O_{12}$:Cr(III)	431, 611	1920	1280	0.56	0.85	~0.04	~0.04	very good	negligible	12
$YAl_3(BO_3)_4$:Cr(III)	421, 600	237	143	0.97	0.57	0.48	0.47	very good	negligible	this work

[a] For Ru-phen embedded into PAN nanobeads. [b] For Eu(tta)$_3$DEADIT embedded into PS-PVP nanobeads.

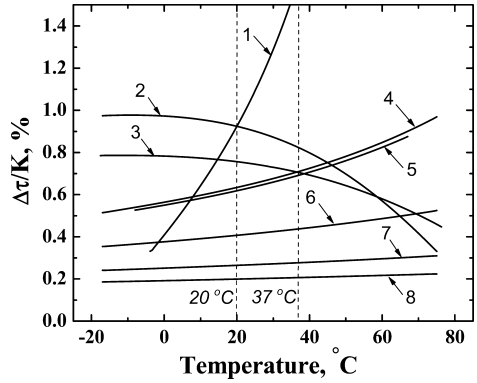

Figure 9. Temperature sensitivities of the visible light-excitable thermographic phosphors and luminescent metal−organic complexes: (1) Eu(tta)$_3$DEADIT in polystyrene; (2)$YAl_3(BO_3)_4:Cr^{3+}$ crystals obtained by high-temperature solution growth (5% Cr(III) in the oxide mixture); (3) $YAl_3(BO_3)_4:Cr^{3+}$ microcrystalline powder (2.5% Cr^{3+}); (4) $Y_3Al_5O_{12}:Cr^{3+}$; (5) Ru-phen in polyacrylonitrile; (6) $MgAl_2O_4:Cr^{3+}$; (7) $Al_2O_3:Cr^{3+}$; and (8) $Mg_4FGeO_6:Mn^{4+}$.

$Y_3Al_5O_{12}$, respectively. In another experiment, the microcrystalline phosphor powders were positioned in a homemade cell and excited in the fluorescence spectrometer in a 60° angle, at two different temperatures, 1 and 60 °C. These results are summarized in Table 1. As can be seen, they are similar to those obtained for the phosphor suspensions. Evidently, Cr(III)-doped YAB shows excellent brightness, which is comparable to that of Mn(IV)-doped Mg_4FGeO_6 (lamp phosphor). Unfortunately, comparison with the established temperature-sensitive organometallic complexes is more complicated due to scattering of microcrystalline powders. Therefore, freeze-dried polymeric beads of Ru-phen in polyacrylonitrile and Eu(tta)$_3$DEADIT in poly(styrene-*block*-vinylpyrrolidone) were used for comparison. At low temperature (1 °C) the brightness of these materials is comparable to that of the Cr(III)-doped $YAl_3(BO_3)_4$. However, in contrast to thermographic phosphors, the brightness of the organometallic complexes deteriorates dramatically if the temperature is increased to 60 °C (Table 1).

As is clearly visible from Figure 9, Cr(III)-doped YABs shows much higher temperature sensitivity compared to other visible light-excitable thermographic phosphors such as Cr(III)-doped $MgAl_2O_4$,[15] Cr(III)-doped Al_2O_3,[14] and Mn(IV)-doped Mg_4FGeO_6.[11] It should be emphasized that although other thermographic phosphors such as ruby- and Mn(IV)-doped Mg_4FGeO_6 are rather established in thermometry, they provide 3−5 times poorer resolution that Cr(III)-doped YAB. At higher temperatures Cr(III)-doped $Y_3Al_5O_{12}$ could compete with YABs in terms of temperature sensitivity, but its performance is compromised by low brightness. As can be seen, ruthenium(II) tris-1,10-phenanthroline complex (Ru-phen)[22,32] has lower temperature sensitivity than Cr(III)-doped YAB. Generally, only luminescent europium(III) complexes such as a visible-light excitable Eu(tta)$_3$DEADIT[33] possess higher temperature sensitivity exceeding 1% per deg. However, at temperatures below room temperature only Cr(III)-doped YAB shows unmatched sensitivity. Moreover, the organic metal−ligand complexes need to be embedded into gas blocking polymers such as polyacrylonitrile, poly(vinylidene chloride-*co*-acrylonitrile), etc. in order to avoid quenching by oxygen. This is not necessary for the phosphors which additionally benefit from excellent photostability and can be continuously excited with LEDs for many days and even weeks without showing any deterioration. On the contrary, all metal complexes are prone to photobleaching, which is often very pronounced for the europium(III) luminophores.[33,34] Table 1 summarizes the properties of the most common probes used in room temperature thermometry. It is evident that the Cr(III)-doped YAB is an excellent alternative to the state of the art thermographic phosphors and luminescent organometallic complexes.

Imaging Applications. Imaging of temperature distribution is of high importance in several applications. Pressure-sensitive paints, particularly, rely on luminescent indicators which are used to monitor the total pressure via oxygen partial pressure.[31] Unfortunately, temperature affects both the luminescence of an oxygen indicator and gas permeability coefficients of a polymer where the indicator is dissolved. To obtain correct pressure values the temperature effect should be compensated for. It is usually achieved by addition of temperature-sensitive metal complexes (commonly immobilized in beads)[26,30] or thermographic phosphor powders[17,29] to the pressure-sensitive paint. Figure 10A shows a photographic image of the sensor coating (Cr(III)-doped YAB dispersed in hydrogel D4), which reveals a very homogeneous layer. This is of course not surprising considering the size of the microcrystalline powder (2.6 ± 0.5 nm). The luminescence decay times (Figure 10B−D) calculated from the images obtained with a gated CCD camera clearly demonstrate the suitability of the material for imaging of temperature distribution on surface. However, it should be considered that the sensitivity of the CCD cameras decreases in the NIR region, which decreases the S/N ratio in the case of Cr(III)-doped YAB.

Cr(III)-Doped $GdAl_3(BO_3)_4$ and Similar Phosphors. Apart from yttrium aluminum borate several similar hosts were reported. It is well-known that such trivalent ions as lanthanum, gadolinium, and lutetium can occupy the yttrium sites and scandium(III) or gallium(III) can substitute aluminum. Thus, fine-tuning of photophysical properties of the Cr(III)-doped borate phosphors might be possible. For example, it was demonstrated[44] that Cr(III)-doped yttrium scandium borate is excitable at longer wavelength than Cr(III)-doped YAB and has bathochromically shifted emission. Both excitation and emission spectra are bathochromically shifted if aluminum is partly substituted by gallium.[47] For both phosphors the intensity of the sharp R-line associated with the $^2E \rightarrow {}^4A_2$ transition is very low. Our preliminary investigations indicate that Cr(III)-doped $YSc_3(BO_3)_4$ and $YGa_3(BO_3)_4$ possess lower brightness than the

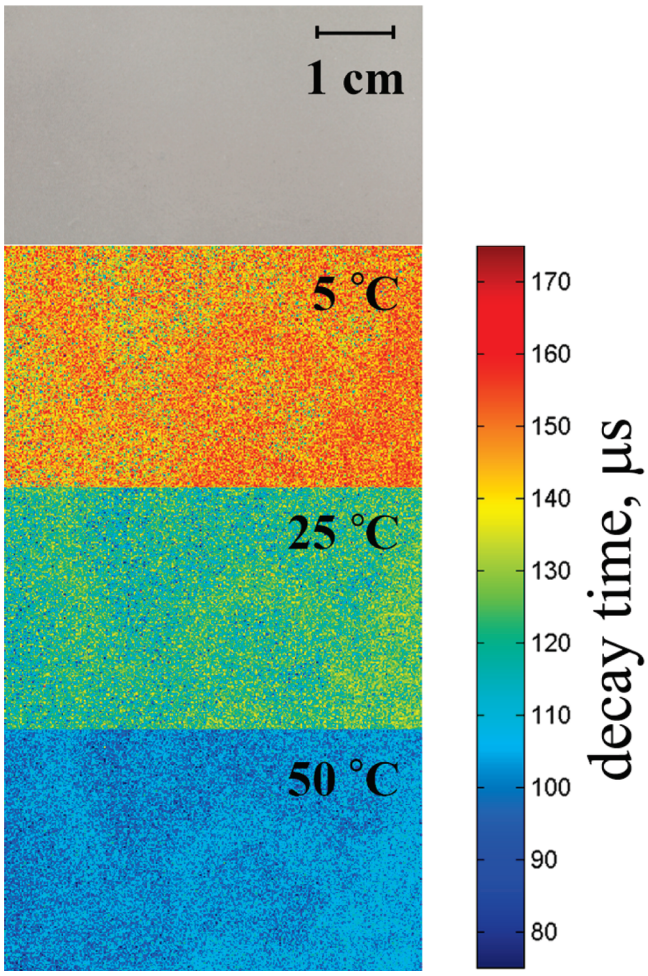

Figure 10. (A) A photographic image of the ~10 μm thick coating (50% w/w of Cr(III)-doped YAB, 2.5% doping, in hydrogel D4). (B−D) Lifetime distribution for the same coating at different temperatures.

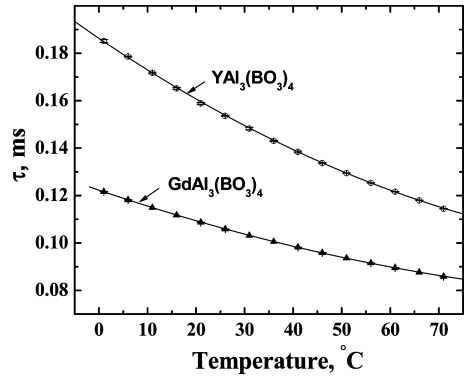

Figure 11. Temperature dependence of the luminescence decay time for Cr(III)-doped $YAl_3(BO_3)_4$ and $GdAl_3(BO_3)_4$ microcrystalline powders (2.5% Cr(III) doping).

respective Cr(III)-doped $YAl_3(BO_3)_4$ with the same doping level. On the other hand, the brightness of Cr(III)-doped gadolinium aluminum borate (GAB) is comparable to that of Cr(III)-doped YAB. The excitation spectra of the two phosphors are very similar (λ_{exc} 423 and 591 nm for GAB and 421 and 600 nm for YAB). However, the luminescence decay time of Cr(III)-doped GAB is significantly lower than that of Cr(III)-doped YAB (Figure 11). The former also shows lower temperature dependence of the decay time. Thus, this phosphor may be suitable for application in dual lifetime referenced (DLR) optical sensors[51] since inertness to chemical and physical parameters (including temperature) is highly desirable in this method.

In conclusion, Cr(III)-doped YAB represents a new type of thermographic phosphor which provides uncompromised solution for sensing and imaging of ambient temperatures. The new material is distinguishable for the following features: (i) excitation in the blue and the red part of the spectrum and compatibility with red laser diodes; (ii) NIR emission; (iii) excellent luminescence brightness; (iv) large temperature coefficients of the decay time at ambient temperatures; (v) uniform brightness in the whole temperature range of interest; and (vi) simplicity in preparation via the combustion route. Compared to luminescent metal−ligand complexes, Cr(III)-doped YAB additionally benefits from chemical and photochemical inertness and the absence of the cross-sensitivity to oxygen. Potential applications include sensing and imaging of temperature in those fields where invasiveness is undesirable and combination of the phosphor with other indicators in temperature-compensated optical chemosensors and pressure-sensitive paints.

Acknowledgment. The financial support from Austrian Science Fund FWF is gratefully acknowledged (Project M-1107-N22).

References and Notes

(1) Fernández-Valdivielso, C.; Egozkue, E.; Matías, I. R.; Arregui, F. G.; Bariáin, C. *Sens. Actuators, B* **2003**, *91*, 231.
(2) Zhao, Y.; Liao, Y. *Sens. Actuators, B* **2002**, *86*, 63.
(3) Grosswig, S.; Hurtig, E.; Kuhn, K. *Geophysics* **1996**, *61*, 1065.
(4) Stefanadis, C.; Tsiamis, E.; Vaina, S.; Toutouzas, K.; Boudoulas, H.; Gialafos, J.; Toutouzas, P. *Am. J. Cardiol.* **2004**, *93*, 207.
(5) Janskya, L.; Vavraa, V.; Janskyb, P.; Kuncc, P.; Knizkovac, I.; Jandovad, D.; Slovacek, K. *J. Therm. Biol.* **2003**, *28*, 429.
(6) Gouterman, M.; Callis, J.; Dalton, L.; Khalil, G.; Mébarki, Y.; Cooper, K. R.; Grenier, M. *Meas. Sci. Technol.* **2004**, *15*, 1986.
(7) Krenzinger, A.; de Andrade, A. C. *Solar Energy* **2007**, *81*, 1025.
(8) Alison, S. W.; Gillies, G. T. *Rev. Sci. Imstrum.* **1997**, *68*, 2615.
(9) Khalid, A. H.; Kontis, K. *Sensors* **2008**, *8*, 5673.
(10) Brübach, J.; Patt, A.; Dreizler, A. *Appl. Phys. B: Lasers Opt.* **2006**, *83*, 499.
(11) Brübach, J.; Feist, J. P.; Dreizler, A. *Meas. Sci. Technol.* **2008**, *19*, 025602.
(12) Aizawa, H.; Katsumata, T.; Kiyokawa, Y.; Nishikawa, T.; Sasagawa, T.; Komuro, S.; Morikawa, T.; Ishizawa, H.; Toba, E. *Measurement* **2006**, *39*, 147.
(13) Aizawa, H.; Ohishi, N.; Ogawa, S.; Katsumata, T.; Komuro, S.; Morikawa, T.; Toba, E. *Rev. Sci. Instrum.* **2002**, *73*, 3656.
(14) Anghel, F.; Illiescu, C.; Grattan, K. T. V.; Palmer, A. W.; Zhang, Z. Y. *Rev. Sci. Instrum.* **1995**, *66*, 2611.
(15) Aizawa, H.; Ohishi, N.; Ogawa, S.; Watanabe, E.; Katsumata, T.; Komuro, S.; Morikawa, T.; Toba, E. *Rev. Sci. Instrum.* **2002**, *73*, 3089.
(16) Aizawa, H.; Uchiyama, H.; Katsumata, T.; Komuro, S.; Morikawa, T.; Ishizawa, H.; Toba, E. *Meas. Sci. Technol.* **2004**, *15*, 1484.
(17) Coyle, L. M.; Gouterman, M. *Sens. Actuators, B* **1999**, *61*, 92.
(18) Yap, S. V.; Ranson, R. M.; Cranton, W. M.; Koutsogeorgis, D. C.; Hix, G. B. *J. Lumin.* **2009**, *129*, 416.
(19) Shen, Y.; Zhao, W.; Sun, T.; Grattan, K. T. V. *Sens. Actuators, A* **2003**, *109*, 53.
(20) Nagl, S.; Wolfbeis, O. S. *Analyst* **2007**, *132*, 507.
(21) Borisov, S. M.; Wolfbeis, O. S. *Anal. Chem.* **2006**, *78*, 5094.
(22) Borisov, S. M.; Vasylevska, A. S.; Krause, Ch.; Wolfbeis, O. S. *Adv. Funct. Mater.* **2006**, *16*, 1536.
(23) Kocincova, A. S.; Borisov, S. M.; Krause, Ch.; Wolfbeis, O. S. *Anal. Chem.* **2007**, *79*, 8486.
(24) Jorge, P. A. S.; Maule, C.; Silva, A. J.; Benrashid, R.; Santos, J. L.; Farahi, F. *Anal. Chim. Acta* **2008**, *606*, 223.
(25) Baleizao, C.; Nagl, S.; Schaferling, M.; Berberan-Santos, M. N.; Wolfbeis, O. S. *Anal. Chem.* **2008**, *80*, 6449.
(26) Stich, M. I. J.; Nagl, S.; Wolfbeis, O. S.; Henne, U.; Schaeferling, M. *Adv. Funct. Mater.* **2008**, *18*, 1399.
(27) Demas, J. N.; DeGraff, B. A.; Coleman, P. B. *Anal. Chem.* **1999**, *71*, 793A.
(28) Zelelow, B.; Khalil, G.; Phelan, G.; Carlson, B.; Gouterman, M.; Callis, J. B.; Dalton, L. R. *Sens. Actuators, B* **2003**, *96*, 304.
(29) Hradil, J.; Davis, C.; Mongey, K.; McDonagh, C.; MacCraith, B. D. *Meas. Sci. Technol.* **2002**, *13*, 1552.

(30) Koese, M. E.; Carrol, B. F.; Schanze, K. S. *Langmuir* **2005**, *21*, 9121.
(31) Wolfbeis, O. S. *Adv. Mater.* **2008**, *20*, 3759.
(32) Liebsch, G.; Klimant, I.; Wolfbeis, O. S. *Adv. Mater.* **1999**, *11*, 1296.
(33) Borisov, S. M.; Klimant, I. *J. Fluoresc.* **2008**, *18*, 581.
(34) Peng, H.; Stich, M. I. J.; Yu, J.; Sun, L.; Fischer, L. H.; Wolfbeis, O. S. *Adv. Mater.* **2009**, *21*, 1.
(35) Uchiyama, S.; Matsumura, Y.; Prasanna de Silva, A.; Iwai, K. *Anal. Chem.* **2003**, *75*, 5926.
(36) Uchiyama, S.; Matsumura, Y.; Prasanna de Silva, A.; Iwai, K. *Anal. Chem.* **2004**, *76*, 1793.
(37) Borisov, S. M.; Mayr, T.; Klimant, I. *Anal. Chem.* **2008**, *80*, 573.
(38) Borisov, S. M.; Nuss, G.; Haas, W.; Saf, R.; Schmuck, M.; Klimant, I. *J. Photochem. Photobiol., A* **2009**, *201*, 128.
(39) Rodriguez-Carvajal, J. *Phys. B* **1993**, *192*, 55. Remarks: For a more recent version see Rodriguez-Carvajal, J. Recent Developments of the Program FULLPROF, in Commission on Powder Diffraction (IUCr).Newsletter (2001), 26, 12−19 (http://journals.iucr.org/iucr-top/comm/cpd/Newsletters/) The complete program and documentation can be obtained in http://www.ill.eu/sites/fullprof/.
(40) Roisnel, T.; Rodriguez-Carvajal, J. *Proceedings of the Seventh European Powder Diffraction Conference (EPDIC 7)*, Barcelona, Spain, May 20−23, 2000; Delhez, R.; Mittenmeijer, E. J., Eds.; 2000; p 118.
(41) Meszaros, G.; Svab, E.; Beregi, E.; Watterich, A.; Toth, M. *Phys. B* **2000**, *276−278*, 310.
(42) Chadeyron, G.; El-Ghozzi, M.; Mahiou, R.; Arbus, A.; Cousseins, J. C. *J. Solid State Chem.* **1997**, *128*, 261.
(43) Mills, A. D. *Inorg. Chem.* **1962**, *1*, 960.
(44) Wang, G.; Gallagher, H. G.; Han, T. P. J.; Henderson, B. *J. Cryst. Growth* **1996**, *163*, 272.
(45) Hong, H. Y. P.; Dwight, K. *Mater. Res. Bull.* **1974**, *9*, 1661.
(46) Wang, G.; Gallagher, H. G.; Han, T. P. J.; Henderson, B. *J. Cryst. Growth* **1995**, *153*, 169.
(47) Iwai, M.; Mori, Y.; Sakaki, T.; Nakai, S.; Sarukura, N.; Liu, Z.; Segawa, Y. *Jpn. J. Appl. Phys.* **1995**, *34*, 2338.
(48) Wen, F.; Li, W.; Liu, Z.; Kim, T.; Yoo, K.; Shin, S.; Moon, J.; Kim, J. K. *Solid State Commun.* **2005**, *133*, 417.
(49) Maia, L. J. Q.; Ferrari, C. R.; Mastelaro, V. R.; Hernandes, A. C.; Ibanez, A. *Solid State Sci.* **2008**, *10*, 1835.
(50) Dominiak-Dzik, G.; Ryba-Romanowski, W.; Grinberg, M.; Beregi, E.; Kovacs, L. *J. Phys.: Condens. Matter* **2002**, *14*, 5229.
(51) Klimant, I.; Huber, C.; Liebsch, G.; Neurauter, G.; Stangelmayer, A.; Wolfbeis, O. S. In *Springer Series in Fluorescence Spectroscopy*; Valeur, B., Brochon, J. C., Eds.; Springer: Berlin, Germany, 2001, *1*, 257.

JP1016467